JOURNAL OF SOLID STATE CHEMISTRY **82**, 109–114 (1989)

Synthesis and Characterization of $Sr(Al,Cr)_{12}O_{19}$ Solid Solution

FELIP SANDIUMENGE

Institut de Ciència de Materials de Barcelona (CSIC) C/Martí i Franquès S/N, 08028 Barcelona, Spain

AND SALVADOR GALÍ

Departament de Cristal-lografia i Mineralogia, Universitat de Barcelona, C/Martí i Franquès S/N, 08028 Barcelona, Spain

Received September 9, 1988; in revised form May 1, 1989

Magnetoplumbite-type crystalline powders with $SrAl_{12-x}Cr_xO_{19}$ composition were synthesized in the range $0 \leq x \leq 4.4$ by two different solid state reactions in air. The limited substitution of Al by trivalent Cr is accompanied by the appearance of a sesquioxide $Al_{2-y}Cr_yO_3$ solid solution and a new cubic phase with composition $3Al_2O_3 \cdot SrCrO_4$. These results are compared with those obtained in the synthesis of $Sr(Fe,Cr)_{12}O_{19}$ and $Sr(Al,Fe)_{12}O_{19}$ solid solutions. Finally, the cation distribution of Al and Cr in the system $Sr(Al,Cr)_{12}O_{19}$–$(Al,Cr)_2O_3$ was obtained from X-ray diffraction profile analysis. The cationic distribution suggests that the solid solution range depends more on the crystal chemistry of the substitution than on the starting compounds used in the synthesis.

Introduction

The magnetoplumbite structure (space group $P6_3/mmc$, $Z = 2$) (*1*) has been widely discussed by several authors; hence only an overview is given here. Five nonequivalent sublattices are present, of which three are octahedral (in Wyckoff notation $2a$, $12k$, and $4f_2$), one is tetrahedral, $4f_1$, and the remaining one indicated by $2b$ was previously described as fivefold coordinated in a trigonal bipyramid (*1*). In $BaFe_{12}O_{19}$, cations placed in such polyhedral experience dynamic disorder between the two adjacent tetrahedra (*2*). The magnetoplumbite structure is described as the superposition of two structural blocks S and R along the c axis. The S block consists of $2a$, $4f_1$, and $12k$, the latter being placed on a mirror plane at the R–S interphase, and $4f_2$ and $2b$ belong to the R block.

The $SrFe_{12-x}Cr_xO_{19}$ solid solution was investigated by several authors by neutron diffraction (*3, 4*) and Mössbauer spectroscopy (*4, 5*), and the $SrFe_{12-x}Al_xO_{19}$ solid solution by X-ray diffraction methods (*6*). In the former case, the solid solution is not complete, the maximum value for the composition parameter being $x \cong 9$. This fact has been explained by considering the difficulty for trivalent Cr to enter both tetrahedral and pentahedral sites. In the second case the solid solution is complete and a marked preference of Al for octahedral sites was observed. We find that, in Sr $(Al,Cr)_{12}O_{19}$, this value is lowered to $\cong 4.4$.

0022-4596/89 $3.00

This behavior can be explained by considering a competition between both cations for octahedral sublattices. The affinity of both cations for these sites generates a marked occupational hierarchy, which suggests that the equilibrium $Sr(Al,Cr)_{12}O_{19}$–$(Al,Cr)_2O_3$ in air is favored by the presence of the octahedral 12*c* sublattice in the sesquioxide. We also show that the solid solution range is not expanded by using different starting compounds in the synthesis in air.

Assuming that Cr^{3+} does not enter into the tetrahedral sites, the substitution of Al by Cr^{3+} in both blocks may be described by the following formulae,

$$\{[Al_{1-p_1}Cr_{p_1}]^{2a}[Al_{3(1-p_2)}Cr_{3p_2}]^{12k/2}[Al_2]^{4f_1}O_8\}^{2+} \quad (1)$$

$$\{[Al_{3(1-p_2)}Cr_{3p_2}]^{12k/2}Al_{1-p_3}Cr_{p_3}]^{2b}[Al_{2(1-p_4)}Cr_{2p_4}]^{4f_2}SrO_{11}\}^{2-} \quad (2)$$

$$p_1 + 6p_2 + p_3 + 2p_4 = x$$

for the S and R blocks, respectively. Here p_i is the population factor associated with site *i*, and superscript 12*k*/2 accounts for the sharing of 12*k* sites between blocks S and R.

Experimental and Calculations

Synthesis

Powder mixtures with composition $SrCO_3 + zCr_2O_3 + (6 - z)Al_2O_3$, $z = 1, 2, 3,$ 4, and 5, were placed in platinum crucibles and heated to 1300°C in air. After each 48 hr, the mixtures were rehomogenized and the completion of the reaction was checked by X-ray diffraction. We shall refer to sample 1, 2 . . . for samples with starting composition $z = 1, 2 \ldots$, respectively.

TABLE I

PHASES APPEARING IN EACH SAMPLE, REFINED CELL PARAMETERS (Å), AND STOICHIOMETRIC COEFFICIENTS

Sample (*z*)	$SrAl_{12-x}Cr_xO_{19}$	$Al_{2-y}Cr_yO_3$	Cubic
1	$x = 1.5$	$y = 0.46$[a]	
	$a = 5.6158(3)$	$a = 4.7964(6)$	
	$c = 22.1854(8)$	$c = 13.1097(8)$	
2	$x = 4.2$	$y = 1.10$[a]	
	$a = 5.6496(3)$	$a = 4.8819(5)$	
	$c = 22.3100(7)$	$c = 13.2754(6)$	
3	$x = 4.4$	$y = 1.28$	
	$a = 5.6661(3)$	$a = 4.9228(2)$	$a = 6.674(2)$
	$c = 22.3623(6)$	$c = 13.4610(3)$	
4	Small quantity	$a = 4.932(1)$	$a = 6.675(2)$
		$c = 13.503(6)$	
5[b]		$a = 4.9456(9)$	Not refined
		$c = 13.544(5)$	

[a] Estimated from cell parameters.

[b] $SrCrO_4$ is also present.

For samples 1 and 2 two final phases were obtained, the $(Cr,Al)_2O_3$ and $Sr(Cr,Al)_{12}O_{19}$ solid solutions. Samples 3 and 4 yielded a new phase which could be easily indexed assuming a primitive cubic lattice. In addition, in sample 5, small amounts of strontium chromate were present. The composition of the cubic phase was obtained by chemical analysis of the solution obtained by dissolving sample 4 in hot diluted HNO_3. The weight of chromate amounts to about 12% of total weight. X-ray diffraction patterns recorded before and after the dissolution indicated that only the cubic chromate disappeared during the process. The chemical analyses give rise to the formula $3Al_2O_3 \cdot SrCrO_4$.

In order to avoid the oxidation of Cr^{3+} to Cr^{6+} through the well-known reaction between $SrCO_3$ and Cr_2O_3, reactions such as $aSrAl_2O_4 + bAl_2O_3 + cCr_2O_3 \rightarrow aSr(Al,Cr)_{12}O_{19}$ $(b + c = 5a)$ were tried. This reaction avoids the presence of free SrO and starts with $SrAl_2O_4$, which forms during the reaction between the single oxides (*7*). However, we obtained the results described in Table I, showing that the system reaches the equilibrium through the coexistence of the above phases independently of the starting materials.

In agreement with von Steinwehr (*8*), the compositions of the sesquioxide in samples

TABLE II

EXPERIMENTAL CONDITIONS EMPLOYED IN X-RAY ANALYSES AND *R*-FACTORS

		Sample
Angular range (2θ in degrees)	27–100	1, 2
	22–100	3
Excluded regions	None	
Step width (2θ in degrees)	0.05	
Count time (sec)	30	1, 2
	24	3

Sample (z)	1		2		3	
R-Factor	hexa	sesq	hexa	sesq	hexa	sesq
R_B[a]	3.75	9.42	4.28	4.92	3.81	4.20
R_P[b]	7.73		7.22		6.85	
R_{WP}[c]	10.1		9.50		8.82	
R_{EXP}	3.52		3.88		4.36	
Total number of Bragg reflections	146	31	147	34	150	36

[a] $R_B = 100 \times (\Sigma_k|`I_k(O)' - I_k(C)|)/\Sigma_k `I_k(O)'$.

[b] $R_B = 100 \times (\Sigma_i|Y_i(O) - Y_i(C)|)/\Sigma_i Y_i(O)$.

[c] $R_{WP} = 100 \times [(\Sigma_i W_i(Y_i(O) - Y_i(C))^2)/\Sigma_i W_i(Y_i(O))^2]^{1/2}$.

4 and 5, $Cr_{1.7}Al_{0.3}O_3$ and $Cr_{1.8}Al_{0.2}O_3$, were determined from the cell parameters.

Diffraction

Recording was performed in a step-scanning mode with a Siemens D500 diffractometer, using CuK_α radiation and a pyrolitic graphite diffracted-beam monochromator. A 0.15° slit detector was used allowing a number of counts per step between 200 (background) and 18000 (maximum). Samples 4 and 5 were studied by conventional X-ray procedure. After appropriate grinding, the samples were prepared by sedimentation from aqueous media over polyvinile chloride membranes (Geilman Sciences, Inc.) in order to decrease preferential orientation of crystallites.

Structure Refinement

In Table II experimental conditions and *R* factors are summarized. Crystal structure refinements were carried out on samples 1, 2, and 3. The pattern profile was refined with the Rietveld method by using the DBW3.2 version of the Wiles and Young program (*9*). Figure 1 shows the experimental X-ray diffraction patterns with fitted profiles, the difference pattern, and the position of diffraction maxima.

Initial structural parameters in sample 1 were taken from the refinement of $SrAl_{10}Fe_2O_{19}$ (*6*) for the hexaferrite-like phase. For the sesquioxide phase, they were taken from Newheim and de Haan (*10*). The background was fitted with a six-parameter function, and the pseudo-Voigt lineshape function (*11*) was used (η oscillates around 0.65). In order to account for preferential orientation corrections, the March function was used (*12, 13*). Samples 1 and 2 were also refined on the basis that they did not contain sesquioxide; however, the *R* factors were lowered when refining both phases simultaneously (the maximum number of parameters varied was 42). The global temperature factor was either refined or determined by trial. No constraints were imposed between fitting parameters and cycles were continued until shifts were 0.06 times the standard deviations of fitting parameters. In all the runs, as expected, no Cr^{3+} was found to occupy the tetrahedral site; hence, its occupation factor was fixed at zero.

Results and Discussion

As the chromium content increases in the starting mixture, the amount of magnetoplumbite-type phase decreases while that of the sesquioxide phase increases. However, the chromoium content in $Sr(Al,Cr)_{12}O_{19}$ remains roughly constant in samples 2 and 3. The quantitative analysis was performed using the relation of the refined scale factors,

$$r_{1,2} = K_1 Vc_1 Z_1 M_1 / K_2 Vc_2 Z_2 M_2, \quad (3)$$

where K_i are the refined scale factors, Vc_i the unit cell volumes, Z_i the number of formula units per unit cell and M_i the molecu-

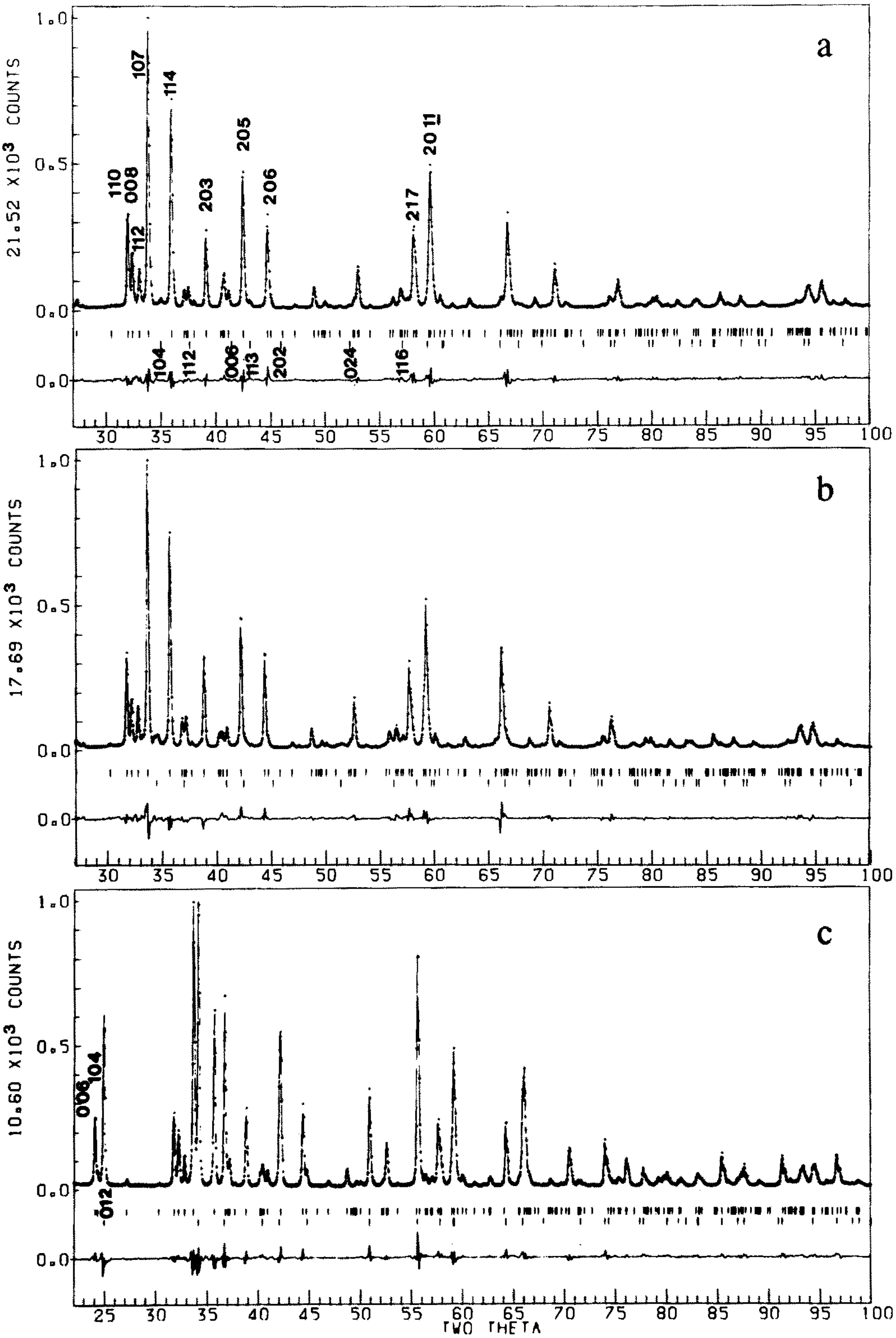

FIG. 1. X-ray diffraction patterns of samples 1 (a), 2 (b), and 3 (c) with positions of diffraction maxima for both phases and difference curve. Upper indices correspond to the magnetoplumbite-type phase.

TABLE III

POPULATION FACTORS FOR Cr^{3+} CATION IN EACH SUBLATTICE

Sample (z)	2*a*	2*b*	12*k*	$4f_2$	12*c* (sesq)
1	0.00(2)	0.04(2)	0.12(1)	0.35(1)	0.23[a]
2	0.28(2)	0.07(2)	0.416(6)	0.71(1)	0.55[a]
3	0.30(3)	0.07(2)	0.45(1)	0.68(2)	0.64(1)

[a] Estimated from cell parameters.

lar weights. Knowing that $X_2 = 100/(1 + r_{1,2})$, application of Eq. (3) for sample 3 leads to 43.9% of sesquioxide.

Cation Distribution in $SrAl_{12-x}Cr_xO_{19}$–$Al_{2-y}Cr_yO_3$, $0 \leq x \leq 4.4$

Population factors and standard deviations for each sublattice in samples 1, 2, and 3 are given in Table III. These results are depicted in Fig. 2a, which indicates that the Cr^{3+} cations preferentially occupy the octahedral sites $4f_2$, 12*k*, and 2*a*, in this order of preference. Furthermore, Fig. 2a also shows that the 2*b* site is occupied to a very low extent by Cr^{3+} and the tetrahedral $4f_1$ site remains unoccupied by Cr^{3+}. The population factors for the octahedral 12*c* sublattice in the sesquioxide suggests a behavior fairly similar to that of the $4f_2$ Cr^{3+} populations in the magnetoplumbite-type structure.

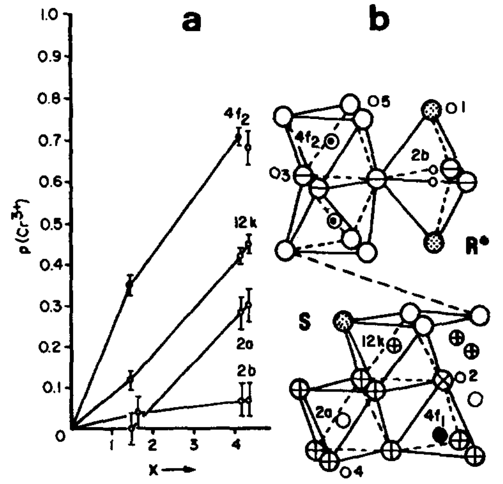

FIG. 2. (a) Variation of the Cr^{3+} population with composition. Error bars represent twice the calculated standard deviation. (b) Partial view of blocks R* and S indicating the relative positions of the five sublattices (modified from Obradors *et al.* (*2*)).

Occupation in Octahedral Sublattices

In the mixture $Sr(Al,Cr)_{12}O_{19}$–$(Al,Cr)_2O_3$, four octahedral sublattices are present. Competition between both cations for the occupation of the octahedral sites arises from the high symmetry of charge distribution and ionic character of Al cation, and from the well-known high crystal field stabilization energy of Cr^{3+} in octahedral sites. Thus, the occupation by Al of the face-sharing octahedra $4f_2$ (3*m*) appears to be less favorable than the occupation of the edge-sharing 12*k* (*m*) and 2*a* (3*m*) octahedra (Fig. 2b). In fact, the 12*c* octahedra (symmetry 3) in the sesquioxide also share faces and show a substitution trend parallel to that of the $4f_2$ octahedra. Hence, in the mixture of both phases, the cation distribution appears to be governed to some extent by symmetry constraints of the octahedral sites present in the system.

In Table IV, some important distances and the mean-square relative distortion of the 12*k* site are listed. It is interesting to compare the constance of the 2*a*–12*k* distances with increasing distortion of the 12*k*

TABLE IV

SOME IMPORTANT DISTANCES[a]

Sample (z)	2*a*–04	2*a*–12*k*	Δ_{12k} ($\times 10^4$)	2*b*–*m*	2*b*–01
1	1.895(1)	2.8959(4)	24.41	0.2800(5)	1.990(1)
2	1.907(2)	2.8954(4)	16.26	0.2880(6)	1.979(1)
3	1.928(1)	2.8995(4)	15.45	0.2660(5)	2.014(1)

[a] 2*b*–*m* refers to the distance from the atom located in 2*b* to the center of the bipyramid, i.e., the deviation from the bipyramidal position, 01 and 04 refer to oxygen atoms (see Fig. 2b), and the mean square relative distortion of the 12*k* octahedra:

$$\Delta_{12k} = (\tfrac{1}{6}) \Sigma_{j=1}^{6} \{[d_{ij} - \langle d_i \rangle]/\langle d_i \rangle\}^2, \quad \langle d_i \rangle = (\tfrac{1}{6}) \Sigma_{j=1}^{6} d_{ij}.$$

octahedra as the Al content increases from sample 3 to sample 1. From substitution of the refined population factors, p_i, in Eqs. (1) and (2), a relative enrichment in Cr of the R block is observed, giving 64.3% of chromium for sample 2.

Occupation in the 2b Site

Bertaut *et al.* (*3*) supposed $x = 8$ in Sr $Fe_{12-x}Cr_xO_{19}$ as the limiting substitution, assuming that Cr^{3+} only enters octahedral sites. Later Obradors *et al.* (*4*) confirmed the inability of Cr^{3+} to enter these sites by means of neutron diffraction and Mössbauer spectroscopy studies on the same solid solution. Despite these results, Rao *et al.* (*5*) suggested a remarkable distortion of the pentahedral environment with occupation of Cr^{3+} in $SrFe_2Cr_{10}O_{19}$ from Mössbauer studies. Furthermore, it is known (*14*) that high spin Cr^{3+} may appear pentacoordinated in trigonal bipyramids. If Cr^{3+} occupy the 2*b* site, a reduction of the 2*b* mirror distance is to be expected, but at this point, our results are not determinant because average distances are not sensitive enough to such small occupations as those we have calculated (see Table III). Indeed, the populations fitted are of the same order of the standard deviations and practically constant for the three compositions (Fig. 2a).

In order to check the reliability of the refinement results, it was observed that major contributions of the 2*b* sublattice to structure factors occur for reflections (110), (008), (112), (104), and (206) and no overlapping exists between the sesquioxide and the magnetoplumbite-type phase lines (except for (206) in sample 3). Hence, the determination of the Cr^{3+} population in the 2*b* site does not seem to be affected to a large extent by overlapping intensities. Furthermore, an increase in 0.5 units of the hexaferrite-like R_B factors was observed by setting to zero the occupancy of Cr^{3+} in the 2*b* site. Thus, possibly small quantities of trivalent chromium actually enter the pentahedral site.

Acknowledgments

The authors thank Miss Concha Domingo for her valuable comments. This work was supported by the Comisión Asesora y Científica of the Government (Project PR84-0831) and CICYT MAT88-0259.

References

1. W. D. Townes, J. H. Fang, and A. S. Perrota, *Z. Kristallogr.* **125,** 437 (1967).

2. X. Obradors, X. Solans, A. Collomb, D. Samaras, J. Rodriguez, M. Pernet, and M. Font-Altaba, *J. Solid State Chem.* **72,** 218 (1988).

3. E. F. Bertaut, A. Deschamps, R. Pauthenet, and S. Pickart, *J. Phys. Radium* **20,** 404 (1959).

4. X. Obradors, A. Isalgue, A. Collomb, M. Pernet, J. Pannetier, J. Rodriguez, J. Tejada, and J. C. Joubert, *IEEE Trans. Magn.* **20,** 1636 (1984).

5. P. M. Rao, A. Gerard, and F. Grandjean, *Phys. Status Solidi A* **54,** 529 (1979).

6. F. Sandiumenge, S. Gali, and J. Rodriguez, *Mat. Res. Bull.* **23,** 685 (1988).

7. M. Medarde, J. Rodriguez, M. Vallet, M. Pernet, X. Obradors, and J. Pannetier, to be published.

8. H. E. von Steinwehr, *Z. Kristallogr.* **125,** 377 (1967).

9. D. B. Wiles and R. A. Young, *J. Appl. Crystallogr.* **14,** 149 (1981).

10. R. E. Newheim and Y. M. de Haan, *Z. Kristallogr.* **117,** 235 (1962).

11. R. A. Young and D. B. Wiles, *J. Appl. Crystallogr.* **15,** 430 (1982).

12. A. March, *Z. Kristallogr.* **81,** 285 (1932).

13. N. A. Dollese, *J. Appl. Crystallogr.* **19,** 267 (1986).

14. F. A. Cotton and G. Wilkinson, "Química Inorgánica Avanzada," 4th ed., p. 785, Ed. Limusa, México, 1986.